

Synthesis and Reactivity of Dialkyl Lutetium Complexes Supported by a Novel Bis(phosphinimine)carbazole Pincer Ligand

Kevin R. D. Johnson and Paul G. Hayes*

Department of Chemistry and Biochemistry, University of Lethbridge, 4401 University Drive, Lethbridge, AB, Canada, T1K 3M4

Received August 20, 2009

The synthesis of a novel bis(phosphinimine) ancillary ligand based on a carbazole framework is described (HL^{Ph} , **4a**; HL^{Pipp} , **4b**; Ph = phenyl, Pipp = *para*-isopropylphenyl). Protonolysis with $\text{Lu}(\text{CH}_2\text{SiMe}_3)_3(\text{THF})_2$ afforded the corresponding lutetium dialkyl complexes ($\text{LuL}^{\text{Ph}}(\text{CH}_2\text{SiMe}_3)_2$, **5a**; $\text{LuL}^{\text{Pipp}}(\text{CH}_2\text{SiMe}_3)_2$, **5b**), which were thermally sensitive and rapidly underwent intramolecular metalative alkane elimination to generate $\text{LuL}^{\text{Ph}*}(\text{CH}_2\text{SiMe}_3)(\text{THF})$, **6a**, and $\text{LuL}^{\text{Pipp}*}(\text{CH}_2\text{SiMe}_3)(\text{THF})$, **6b**, as highly reactive intermediates. Complexes **6a** and **6b** further decomposed, cleanly generating doubly metalated complexes $\text{LuL}^{\text{Ph}^{**}}(\text{THF})$, **7a**, and $\text{LuL}^{\text{Pipp}^{**}}(\text{THF})$, **7b**, respectively, as the thermodynamic products. Kinetic analysis of the decomposition of **5a** revealed a first-order mechanism with activation parameters $\Delta H^\ddagger = 19.2(1) \text{ kcal} \cdot \text{mol}^{-1}$ and $\Delta S^\ddagger = -8.2(2) \text{ cal} \cdot \text{K}^{-1} \cdot \text{mol}^{-1}$. Compounds **4a**, **4b**, **6b**, and **7b** were characterized by single-crystal X-ray diffraction studies.

Introduction

Although organometallic chemistry of group 3 and lanthanide metals has received an increasing amount of attention over the past two decades, it still lags significantly behind that of the transition metals.¹ This is in part due to the highly ionic nature of the lanthanides and reactivity issues such as ligand redistribution and “ate” complex formation.² Largely these challenges can be overcome through the use of appropriate lanthanide precursors that incorporate sufficient steric bulk to saturate the coordination sphere of the metal³ or, alternatively, with ancillary ligands that impose a multidentate

coordination mode.^{2b,4} Despite this, the lack of adequate ancillaries for supporting these metals has drastically limited their applications in organometallic processes such as olefin polymerization,⁵ catalytic hydroamination,⁶ and C–H bond activation.⁷ While the cyclopentadienyl ligand system has been extremely influential in the development

*Corresponding author. E-mail: p.hayes@uleth.ca.

(1) (a) Hou, Z.; Wakatsuki, Y. *Organometallic Complexes of Scandium, Yttrium, and the Lanthanides*. In *Science of Synthesis*; Imamoto, T., Noyori, R., Eds.; Thieme: Stuttgart, 2002; Vol. 2, pp 849–942. (b) Edelmann, F. T. *Coord. Chem. Rev.* **2009**, 253, 343–409. (c) Edelmann, F. T. *Angew. Chem., Int. Ed. Engl.* **1995**, 34, 2466–2488.

(2) (a) Anwender, R. *Top. Organomet. Chem.* **1999**, 2, 1–61. (b) Piers, W. E.; Emslie, D. J. H. *Coord. Chem. Rev.* **2002**, 233–234, 131–155. (c) Raymond, K. N.; Eigenbrot, C. W., Jr. *Acc. Chem. Res.* **1980**, 13, 276–283. (d) Piers, W. E.; Shapiro, P. J.; Bunel, E. E.; Bercaw, J. E. *Synlett* **1990**, 74–84. (e) Schumann, H.; Müller, J. *J. Organomet. Chem.* **1979**, 169, C1–C4.

(3) (a) Anwender, R.; Herrmann, W. A. *Top. Curr. Chem.* **1996**, 179, 1–32. (b) Masuda, J. D.; Jantunen, K. C.; Scott, B. L.; Kiplinger, J. L. *Organometallics* **2008**, 27, 1299–1304. (c) Masuda, J. D.; Jantunen, K. C.; Scott, B. L.; Kiplinger, J. L. *Organometallics* **2008**, 27, 803–806. (d) Meyer, N.; Roesky, P. W.; Bambirra, S.; Meetsma, A.; Hessen, B.; Saliu, K.; Takats, J. *Organometallics* **2008**, 27, 1501–1505. (e) Yan, K.; Pawlikowski, A. V.; Ebert, C.; Sadow, A. D. *Chem. Commun.* **2009**, 656–658. (f) Emslie, D. J. H.; Piers, W. E.; Parvez, M.; McDonald, R. *Organometallics* **2002**, 21, 4226–4240. (g) Power, P. P. *J. Organomet. Chem.* **2004**, 689, 3904–3919.

(4) (a) Mountford, P.; Ward, B. D. *Chem Commun.* **2003**, 1797–1803. (b) Chomitz, W. A.; Arnold, J. *Chem.—Eur. J.* **2009**, 15, 2020–2030. (c) Hajela, S.; Schaefer, W. P.; Bercaw, J. E. *J. Organomet. Chem.* **1997**, 532, 45–53. (d) Shao, P.; Berg, D. J.; Bushnell, G. W. *Inorg. Chem.* **1994**, 33, 3452–3458. (e) Lee, L.; Berg, D. J.; Einstein, F. W.; Batchelor, R. J. *Organometallics* **1997**, 16, 1819–1821. (f) Cheng, J.; Saliu, K.; Kiel, G. Y.; Ferguson, M. J.; McDonald, R.; Takats, J. *Angew. Chem., Int. Ed.* **2008**, 47, 4910–4913.

(5) (a) Hayes, P. G.; Piers, W. E.; McDonald, R. *J. Am. Chem. Soc.* **2002**, 124, 2132–2133. (b) Yu, N.; Nishiura, M.; Li, X.; Xi, Z.; Hou, Z. *Chem. Asian J.* **2008**, 3, 1406–1414. (c) Watson, P. L. *J. Am. Chem. Soc.* **1982**, 104, 337–339. (d) Hou, Z.; Luo, Y.; Li, X. *J. Organomet. Chem.* **2006**, 691, 3114–3121. (e) Gromada, J.; Carpentier, J.-F.; Mortreux, A. *Coord. Chem. Rev.* **2004**, 248, 397–410. (f) Nakayama, Y.; Yasuda, H. *J. Organomet. Chem.* **2004**, 689, 4489–4498. (g) Hou, Z.; Wakatsuki, Y. *Coord. Chem. Rev.* **2002**, 231, 1–22. (h) Edelmann, F. T. *Top. Curr. Chem.* **1996**, 179, 247–276. (i) Gibson, V. C.; Spitzmesser, S. K. *Chem. Rev.* **2003**, 103, 283–315.

(6) (a) Hong, S.; Marks, T. J. *Acc. Chem. Res.* **2004**, 37, 673–686. (b) Hultsch, K. C. *Adv. Synth. Catal.* **2005**, 347, 367–391. (c) Hultsch, K. C.; Gribkov, D. V.; Hampel, F. *J. Organomet. Chem.* **2005**, 690, 4441–4452. (d) Bürgstein, M. R.; Berberich, H.; Roesky, P. W. *Chem.—Eur. J.* **2001**, 7, 3078–3085. (e) Lauterwasser, F.; Hayes, P. G.; Bräse, S.; Piers, W. E.; Schafer, L. L. *Organometallics* **2004**, 23, 2234–2237. (f) Stanlake, L. J. E.; Schafer, L. L. *Organometallics* **2009**, 28, 3990–3998. (g) Bambirra, S.; Tsurugi, H.; van Leusen, D.; Hessen, B. *Dalton Trans.* **2006**, 1157–1161. (h) Bambirra, S.; Meetsma, A.; Hessen, B. *Organometallics* **2006**, 25, 3454–3462. (i) Gagné, M. R.; Stern, C. L.; Marks, T. J. *J. Am. Chem. Soc.* **1992**, 118, 275–294. (j) Müller, T. E.; Hultsch, K. C.; Yus, M.; Foubelo, F.; Tada, M. *Chem. Rev.* **2008**, 108, 3795–3892. (k) Pohlki, F.; Doye, S. *Chem. Soc. Rev.* **2003**, 32, 104–114. (l) Müller, T. E.; Beller, M. *Chem. Rev.* **1998**, 98, 675–703.

(7) (a) Arndtsen, B. A.; Bergman, R. G.; Mobley, T. A.; Petersen, T. H. *Acc. Chem. Res.* **1995**, 28, 154–162. (b) Watson, P. L.; Parshall, G. W. *Acc. Chem. Res.* **1985**, 18, 51–56. (c) Labinger, J. A.; Bercaw, J. E. *Nature* **2002**, 417, 507–514. (d) Sadow, A. D.; Tilley, T. D. *Angew. Chem., Int. Ed.* **2003**, 42, 803–805. (e) Sadow, A. D.; Tilley, T. D. *J. Am. Chem. Soc.* **2005**, 127, 643–656. (f) Scott, J.; Basuli, F.; Fout, A. R.; Huffman, J. C.; Mindiola, D. J. *Angew. Chem., Int. Ed.* **2008**, 47, 8502–8505. (g) Jantunen, K. C.; Scott, B. L.; Gordon, J. C.; Kiplinger, J. L. *Organometallics* **2007**, 26, 2777–2781. (h) Booij, M.; Deelman, B.-J.; Duchateau, R.; Postma, D. S.; Meetsma, A.; Teuben, J. H. *Organometallics* **1993**, 12, 3531–3540. (i) Watson, P. L. *J. Am. Chem. Soc.* **1983**, 105, 6491–6493. (j) Rothwell, I. P. *Polyhedron* **1985**, 4, 177–200. (k) Duchateau, R.; van Wee, C. T.; Teuben, J. H. *Organometallics* **1996**, 15, 2291–2302.

of organolanthanide chemistry,⁸ it is limited in the extent to which it can be electronically or sterically tuned.⁹ Thus, the development of more versatile ancillary ligands may provide access to metal complexes with unique structure, reactivity, and enhanced catalytic activity. Herein, we report the synthesis of a novel family of monoanionic carbazole-based pincer ligands and their ability to support well-defined monomeric organolanthanide complexes.

Results and Discussion

Ligand Synthesis and Characterization. A novel monoanionic ligand has been prepared whereby two phosphinimine donors have been installed at the 1 and 8 positions of a rigid 3,6-dimethylcarbazole (dmc) backbone. The presence of polar phosphinimine subunits is desirable, as they have been shown to provide ancillary ligands with enhanced capacity for electronic donation.^{10–12} Furthermore, the phosphinimine functionality allows for a high degree of steric and electronic tunability through adjustment of R groups attached at the phosphorus and nitrogen atoms. In particular, the incorporation of sufficient steric bulk may assist in

blocking Lewis bases such as tetrahydrofuran (THF) from binding to the metal center. The presence of sterically demanding groups can also help to reduce the potential for dimerization; however, the degree of incorporated bulk must be carefully selected so as to not completely inhibit reactivity at the metal center.

The high-yielding synthesis of the dmc-based ancillary is outlined in Scheme 1. From 1,8-dibromo-3,6-dimethylcarbazole,¹³ N-protection with *tert*-butoxycarbonyl afforded **1**, which was lithiated and allowed to react with chlorodiphenylphosphine to generate the corresponding diphosphine **2**. Removal of the protecting group was efficiently achieved under thermal conditions¹⁴ (160 °C for 4.5 h), liberating deprotected compound **3**. The synthesis of the desired proteo ligand (HL^{Ph}, **4a**; HL^{Pipp}, **4b**; Ph = phenyl; Pipp = *para*-isopropylphenyl) was completed by reaction of **3** with an appropriate aryl azide under standard Staudinger conditions,¹⁵ installing the phosphinimine functionality with concomitant loss of N₂. This four-step synthetic pathway is highly efficient with overall yields of 73% (**4a**) and 53% (**4b**).

Single crystals of **4a** suitable for an X-ray diffraction study were readily obtained upon recrystallization from a benzene solution layered with pentane at ambient temperature. The molecular structure of **4a** is illustrated in Figure 1 as a thermal ellipsoid plot. Ligand **4a** was designed to chelate metals in a tridentate motif with N1, N2, and N3 occupying a common plane with the aromatic dmc backbone. In the solid state, N1 indeed lies approximately within the same plane as the dmc backbone (N1–P1–C1–C12 torsion angle of –11.1(4)°). However, N3 lies significantly out of this plane with an N3–P2–C8–C9 torsion angle of 68.4(4)°. The rotation of the P2–N3 arm out of the plane of the dmc backbone is likely due to steric interactions between the two *N*-phenyl groups on the phosphinimine moiety. It is possible that in the solid state N1 lies within the plane of the dmc backbone due to the hydrogen-bonding interaction that exists between it and H2C. The distance between the donor and acceptor nitrogen atoms in the N2–H2C···N1 interaction in **4a** is 2.789(5) Å.

Similar to **4a**, single crystals of **4b** were obtained from a concentrated benzene solution layered with pentane. The molecular structure of **4b**, as determined from an X-ray diffraction experiment, is depicted in Figure 2. Analogous to that described for **4a**, ligand **4b** has one nitrogen donor (N1) lying in the same plane as the dmc backbone and one (N3) out of the plane. The N1–P1–C1–C12 and N3–P2–C8–C9 torsion angles of 7.8(2)° and –70.7(2)°, respectively, correspond well with that observed for **4a**. In comparison to that of **4a**, the N3 group in **4b** is rotated about 2° further out of plane from the aromatic backbone, while the N1 group is approximately 2° closer to the plane of the dmc backbone. This small, but statistically relevant difference may be attributed to the presence of the isopropyl groups in the *para* positions of the *N*-aryl rings of **4b**, which create slightly greater steric repulsion between the *N*-aryl rings. It is notable that only minor differences in the geometry of **4a** and **4b** are observed, a fact that correlates well with

(8) (a) Schumann, H.; Meese-Marktscheffel, J. A.; Esser, L. *Chem. Rev.* **1995**, *95*, 865–986. (b) Evans, W. J.; Davis, B. L. *Chem. Rev.* **2002**, *102*, 2119–2136. (c) Evans, W. J. *Inorg. Chem.* **2007**, *46*, 3435–3449.

(9) Examples of unique reactivity achieved through tuning of the Cp ligand: (a) Sun, J.; Berg, D. J.; Twamley, B. *Organometallics* **2008**, *27*, 683–690. (b) Evans, W. J.; Kozimor, S. A.; Ziller, J. W. *J. Am. Chem. Soc.* **2003**, *125*, 14264–14265. (c) Evans, W. J.; Kozimor, S. A.; Ziller, J. W. *Inorg. Chem.* **2005**, *44*, 7960–7969. (d) Beetsma, D. J.; Meetsma, A.; Hessen, B.; Teuben, J. H. *Organometallics* **2003**, *22*, 4372–4374. (e) Evans, W. J.; Allen, N. T.; Ziller, J. W. *J. Am. Chem. Soc.* **2001**, *123*, 7927–7928. (f) Evans, W. J.; Allen, N. T.; Ziller, J. W. *Angew. Chem., Int. Ed.* **2002**, *41*, 359–361. (g) Jaroschik, F.; Nief, F.; Le Goff, X.-F.; Ricard, L. *Organometallics* **2007**, *26*, 1123–1125. (h) Jaroschik, F.; Nief, F.; Le Goff, X.-F.; Ricard, L. *Organometallics* **2007**, *26*, 3552–3558. (i) Jaroschik, F.; Momin, A.; Nief, F.; Le Goff, X.-F.; Deacon, G. B.; Junk, P. C. *Angew. Chem., Int. Ed.* **2009**, *48*, 1117–1121. (j) Meyer, G. *Angew. Chem., Int. Ed.* **2008**, *47*, 4962–4964. (k) Deacon, G. B.; Forsyth, C. M.; Jaroschik, F.; Junk, P. C.; Kay, D. L.; Maschmeyer, T.; Masters, A. F.; Wang, J.; Field, L. D. *Organometallics* **2008**, *27*, 4772–4778. (l) Ruspic, C.; Moss, J. R.; Schürmann, M.; Harder, S. *Angew. Chem., Int. Ed.* **2008**, *47*, 2121–2126.

(10) (a) Aparna, K.; Ferguson, M.; Cavell, R. G. *J. Am. Chem. Soc.* **2000**, *122*, 726–727. (b) Cavell, R. G.; Kamalesh Babu, R. P.; Aparna, K. J. *J. Organomet. Chem.* **2001**, *617*, 158–169. (c) Gamer, M. T.; Dehnen, S.; Roesky, P. W. *Organometallics* **2001**, *20*, 4230–4236. (d) Gamer, M. T.; Roesky, P. W. *J. Organomet. Chem.* **2002**, *647*, 123–127. (e) Zulus, A.; Panda, T. K.; Gamer, M. T.; Roesky, P. W. *Chem. Commun.* **2004**, 2584–2585. (f) Panda, T. K.; Zulus, A.; Gamer, M. T.; Roesky, P. W. *Organometallics* **2005**, *24*, 2197–2202. (g) Panda, T. K.; Zulus, A.; Gamer, M. T.; Roesky, P. W. *J. Organomet. Chem.* **2005**, *690*, 5078–5089. (h) Gamer, M. T.; Rastätter, M.; Roesky, P. W.; Steffens, A.; Glanz, M. *Chem.—Eur. J.* **2005**, *11*, 3165–3172. (i) Rastätter, M.; Zulus, A.; Roesky, P. W. *Chem. Commun.* **2006**, 874–876. (j) Rastätter, M.; Zulus, A.; Roesky, P. W. *Chem.—Eur. J.* **2007**, *13*, 3606–3616. (k) Wiecko, M.; Roesky, P. W.; Burlakov, V. V.; Spannenberg, A. *Eur. J. Inorg. Chem.* **2007**, 876–881. (l) Gamer, M. T.; Roesky, P. W.; Palard, I.; Le Hellaye, M.; Guillaume, S. M. *Organometallics* **2007**, *26*, 651–657. (m) Wiecko, M.; Roesky, P. W. *Organometallics* **2009**, *28*, 1266–1269. (n) Hill, M. S.; Hitchcock, P. B. *Dalton Trans.* **2003**, 4570–4571. (o) Liddle, S. T.; McMaster, J.; Green, J. C.; Arnold, P. L. *Chem. Commun.* **2008**, 1747–1749. (p) Mills, D. P.; Cooper, O. J.; McMaster, J.; Lewis, W.; Liddle, S. T. *Dalton Trans.* **2009**, 4547–4555.

(11) (a) Liu, B.; Cui, D.; Ma, J.; Chen, X.; Jing, X. *Chem.—Eur. J.* **2007**, *13*, 834–845. (b) Liu, B.; Liu, X.; Cui, D.; Liu, L. *Organometallics* **2009**, *28*, 1453–1460. (c) Conroy, K. D.; Piers, W. E.; Parvez, M. J. *Organomet. Chem.* **2008**, *693*, 834–846.

(12) (a) Wheaton, C. A.; Ireland, B. J.; Hayes, P. G. *Organometallics* **2009**, *28*, 1282–1285. (b) Zhu, D.; Budzelaar, P. H. M. *Organometallics* **2008**, *27*, 2699–2705. (c) Welch, G. C.; Piers, W. E.; Parvez, M.; McDonald, R. *Organometallics* **2004**, *23*, 1811–1818. (d) Li, Y.; Wang, Z. *Organometallics* **2002**, *21*, 4641–4647. (e) Al-Benna, S.; Sarsfield, M. J.; Thornton-Pett, M.; Ormsby, D. L.; Maddox, P. J.; Brès, P.; Bochmann, M. *J. Chem. Soc., Dalton Trans.* **2000**, 4247–4257. (f) Courtenay, S.; Walsh, D.; Hawkeswood, S.; Wei, P.; Das, A. K.; Stephan, D. W. *Inorg. Chem.* **2007**, *46*, 3623–3631.

(13) Britovsek, G. J. P.; Gibson, V. C.; Hoarau, O. D.; Spitzmesser, S. K.; White, A. J. P.; Williams, D. J. *Inorg. Chem.* **2003**, *42*, 3454–3465.

(14) Rawal, V. H.; Cava, M. P. *Tetrahedron Lett.* **1985**, *26*, 6141–6142.

(15) (a) Meyer, J.; Staudinger, H. *Helv. Chim. Acta* **1919**, *2*, 635–646. (b) Alajarin, M.; Lopez-Leonardo, C. L.; Llamas-Lorente, P. L.; Bautista, D. *Synthesis* **2000**, *14*, 2085–2091.

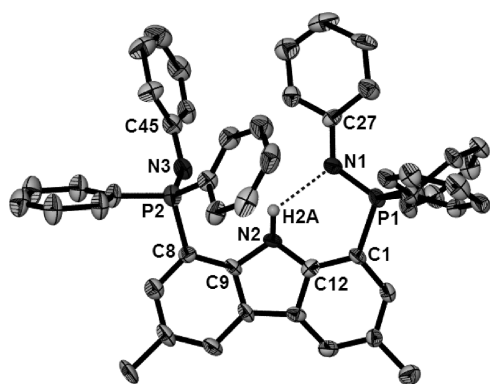
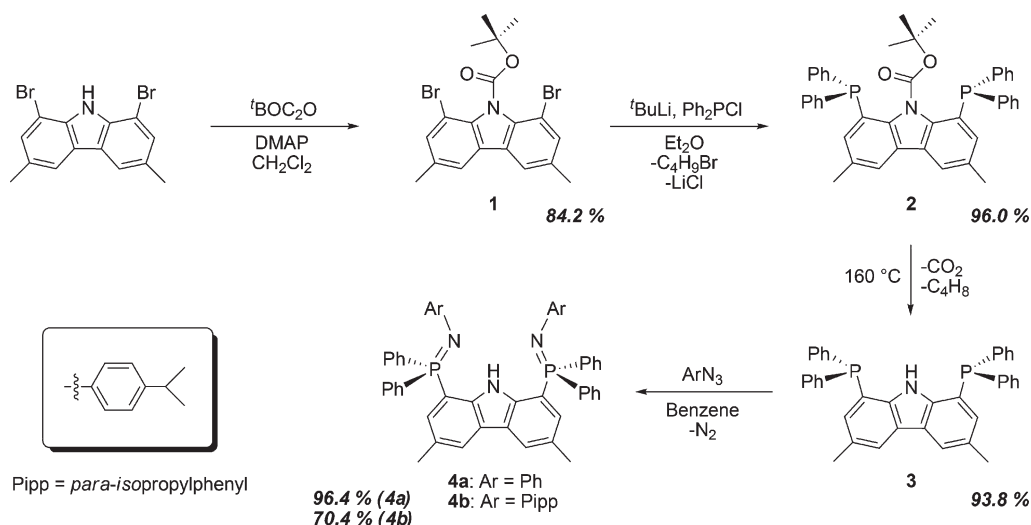
Scheme 1. Synthesis of (ArN=PPh₂)₂(dmc) Ancillary Ligand **4**

Figure 1. Thermal ellipsoid plot (50% probability) of HL^{Ph} (**4a**) with hydrogen atoms (except H2A) and solvent molecules of crystallization omitted for clarity. Selected bond distances (Å) and angles (deg): P1–N1 = 1.581(4), P2–N3 = 1.570(4), N1–P1–C1 = 107.2(2), N3–P2–C8 = 106.0(2), C27–N1–P1 = 126.7(3), C45–N3–P2 = 131.3(4).

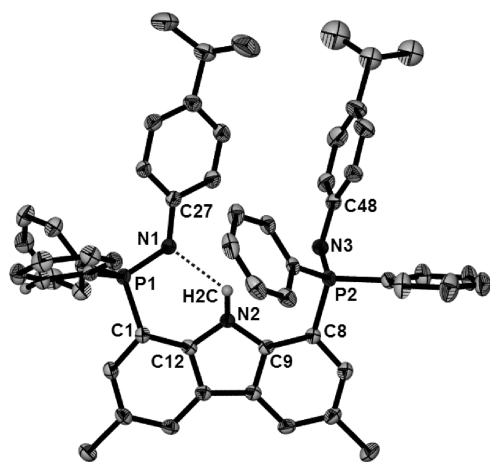
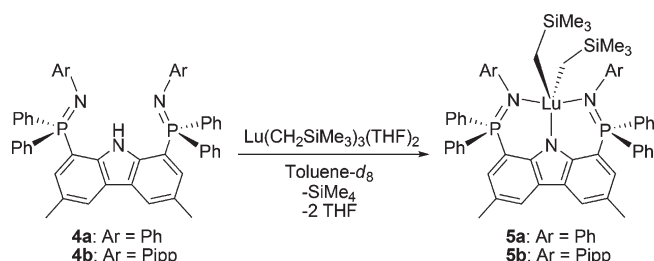


Figure 2. Thermal ellipsoid plot (50% probability) of HL^{Pipp} (**4b**) with hydrogen atoms (except H2C) and solvent molecules of crystallization omitted for clarity. Selected bond distances (Å) and angles (deg): P1–N1 = 1.574(2), P2–N3 = 1.575(2), N1–P1–C1 = 105.3(1), N3–P2–C8 = 106.8(1), C27–N1–P1 = 128.8(2), C48–N3–P2 = 127.0(2).

Scheme 2. Synthesis of Organolutetium Complexes **5a** and **5b**

the identical reaction rates of ligand metalation observed for complexes **5a** and **5b** (*vide infra*).

Proteo ligands **4a** and **4b** are both C_{2v} symmetric on the NMR time scale. Each ligand exhibits a sharp singlet (δ 5.41, **4a**; δ 11.7, **4b**) in its $^{31}\text{P}\{^1\text{H}\}$ NMR (CDCl_3) spectrum. The ^1H NMR spectrum of **4a** (CDCl_3) has a single methyl resonance at δ 2.44, a broad NH peak at δ 11.8, and an expectedly complicated aromatic region. Similarly, the ^1H NMR spectrum of **4b** (CDCl_3) displays a singlet at δ 2.45 corresponding to the symmetric methyls of the dmc backbone and a broad NH signal at δ 11.7. The ^1H NMR spectrum of **4b** also features isopropyl resonances at δ 2.74 (sp, CH) and δ 1.17 (d, CH₃) in addition to a well-defined AB spin pattern (δ 6.74, d; δ 6.64, d) corresponding to protons on the *N*-aryl rings.

Organolutetium Reactivity. Complexation with lutetium was readily achieved via the alkane elimination reaction of $\text{Lu}(\text{CH}_2\text{SiMe}_3)_3(\text{THF})_2$ with **4a** or **4b** (Scheme 2). When equimolar quantities of **4** and $\text{Lu}(\text{CH}_2\text{SiMe}_3)_3(\text{THF})_2$ were reacted in cold (-78°C) toluene- d_8 , the corresponding dialkyl metal complexes $\text{LuL}^{\text{Ph}}(\text{CH}_2\text{SiMe}_3)_2$, **5a**, and $\text{LuL}^{\text{Pipp}}(\text{CH}_2\text{SiMe}_3)_2$, **5b**, began to cleanly form as highly thermally sensitive compounds. Upon warming the solution to 0°C , complete conversion to dialkyl **5** was achieved, as evidenced by consumption of the sparingly soluble proteo ligand and formation of a clear yellow solution. Accordingly, when the reaction was monitored *in situ*, the generation of 1 equiv of tetramethylsilane was observed by ^1H NMR spectroscopy. Due to the thermal sensitivity of dialkyl species **5a** and **5b**, neither complex could be isolated as a pure solid. All attempts to do so resulted in samples contaminated with the thermodynamic decomposition product **7** (*vide infra*). However, both complexes were quantitatively generated

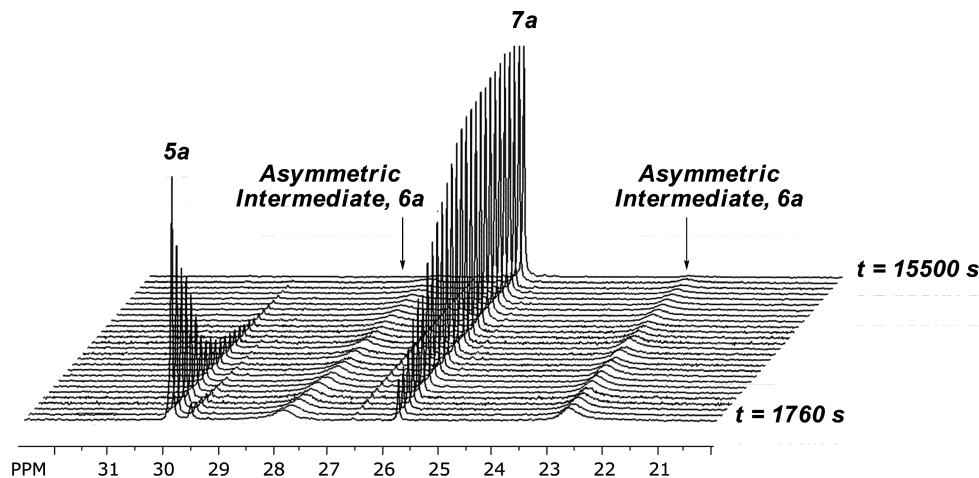
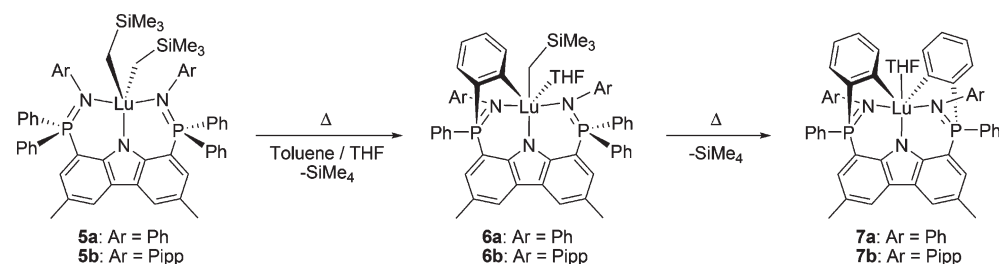


Figure 3. Stacked plot of $^{31}\text{P}\{^1\text{H}\}$ NMR spectra (toluene- d_8) depicting the decomposition of **5a** to **7a** (via intermediate **6a**) at 293.5 K from $t = 1760$ s to $t = 15500$ s.

Scheme 3. Intramolecular Decomposition of Dialkyl Complex **5** to Doubly Metalated Complex **7**



in situ at low temperature and used in this form to further investigate reactivity. Complexes **5a** and **5b** were fully characterized by multinuclear NMR spectroscopy at low temperature with no sign of decomposition over the course of the experiments.

The ^1H NMR spectra of **5** in toluene- d_8 exhibit diagnostic methyl and methylene resonances upfield of 0 ppm for the protons of the trimethylsilylmethyl groups (**5a**, 271.3 K: δ -0.06 (CH_3), -0.79 (CH_2); **5b**, 249.1 K: δ -0.01 (CH_3), -0.72 (CH_2)). Upon cooling solutions of **5a** or **5b** below -60 °C the two trimethylsilylmethyl moieties become inequivalent with splitting of the methylene resonances, indicating a reduction in molecular symmetry from C_{2v} to C_s . In the $^{31}\text{P}\{^1\text{H}\}$ NMR spectra (toluene- d_8), a significant downfield shift of the phosphinimine resonance is observed upon complexation with lutetium (**5a**, 271.3 K: δ 29.6; **5b**, 249.1 K: δ 29.4). As the phosphinimine functionality is highly sensitive to its coordination environment, the large downfield shift is indicative of complexation with the electropositive lutetium center.^{10–12} In addition, the sharp single resonance in the $^{31}\text{P}\{^1\text{H}\}$ NMR spectrum corroborates that the ancillary is bound to lutetium in a κ^3 -coordination mode. Although 2 equiv of THF are present in the *in situ*-generated reaction mixture, it appears that the dialkyl lutetium complex is five-coordinate with no THF donors bound to the metal. Specifically, toluene- d_8 solutions of **5** at temperatures between -40 and 0 °C (the range in which **5** is relatively thermally stable) exhibit resonances in the ^1H and $^{13}\text{C}\{^1\text{H}\}$ NMR spectra consistent with free THF.

At temperatures above 0 °C, toluene solutions of **5** undergo two sequential intramolecular metalative alkane eliminations whereby both alkyl groups are liberated as RH through

a σ -bond metathesis pathway with the *ortho* C–H bonds of the adjacent *P*-phenyl rings. Upon monitoring the decomposition of **5** by ^1H and $^{31}\text{P}\{^1\text{H}\}$ NMR spectroscopy, the formation of an asymmetric intermediate with C_1 symmetry was observed (Scheme 3). This transient species, assigned as monometalated complex **6**, then undergoes a second intramolecular σ -bond metathesis process with a phenyl group from the other phosphinimine phosphorus (*vide infra*), releasing a second equivalent of tetramethylsilane. The final C_2 symmetric products **7a** and **7b** are the result of a rare double-metalation process. These κ^5 -bound lutetium diaryl species consist of two six-membered metallacycles complete with bridging phenyl rings.

The loss of symmetry in the final thermodynamic products, **7a** and **7b**, compared to the initial dialkyl complexes (**5a** and **5b**), was difficult to ascertain through ^1H NMR spectroscopy due to overlapping signals in the aromatic region of the spectrum. However, $^{13}\text{C}\{^1\text{H}\}$ NMR spectroscopy proved to be diagnostic in this regard. The metalated *ipso* carbon attached directly to lutetium is highly deshielded and resonates far downfield as a doublet of doublets at δ 204.6 (dd, $^2J_{\text{PC}} = 41.2$ Hz, $^4J_{\text{PC}} = 1.1$ Hz, **7a**) and δ 204.7 ($^2J_{\text{PC}} = 40.9$ Hz, $^4J_{\text{PC}} = 1.2$ Hz, **7b**). Such values correspond well with the shifts reported for other neutral lutetium aryl species such as $\text{LuPh}_3(\text{THF})_2$ (δ 198.7, benzene- d_6),¹⁶ $\text{Lu}(p\text{-tol})_3(\text{THF})_2$ (δ 195.2, benzene- d_6),¹⁶ $\text{Lu}(\text{C}_6\text{H}_4\text{-}p\text{-Et})_3(\text{THF})_2$ (δ 194.2, benzene- d_6),¹⁶ $(\text{Cp}^*)_2\text{LuPh}$ (δ 198.5, cyclohexane- d_{12}),¹⁷ and $\text{Lu}(o\text{-C}_6\text{H}_4\text{CH}_2\text{NMe}_2)_3$ (δ 196.7, benzene- d_6).¹⁸

(16) Zeimentz, P. M.; Okuda, J. *Organometallics* **2007**, *26*, 6388–6396.

(17) Watson, P. L. *J. Chem. Soc., Chem. Commun.* **1983**, 276–277.

(18) Wayda, A. L.; Atwood, J. L.; Hunter, W. E. *Organometallics* **1984**, *3*, 939–941.

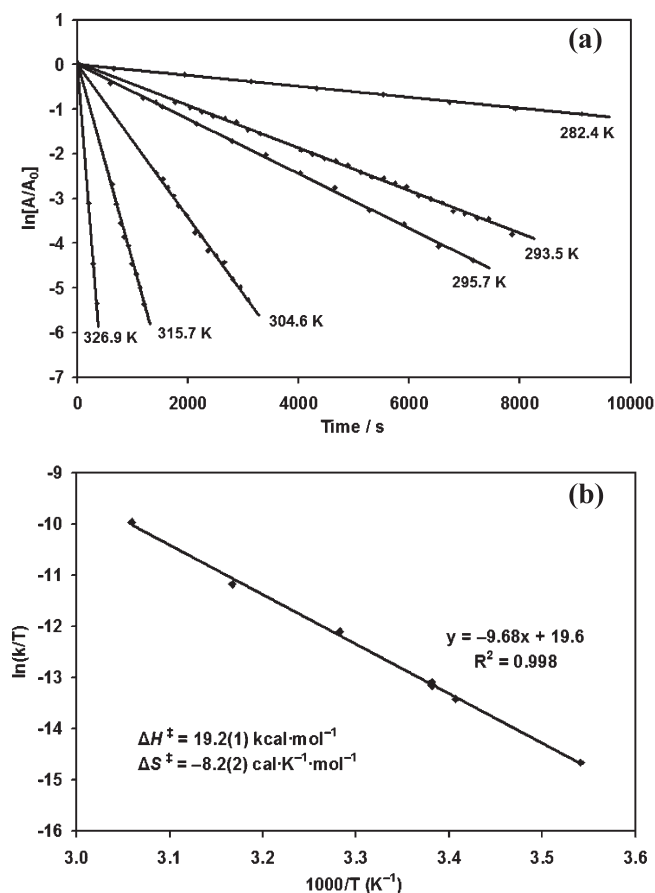


Figure 4. (a) First-order plots of the metalation of **5a** at various temperatures. (b) Eyring plot for the metalation of **5a**.

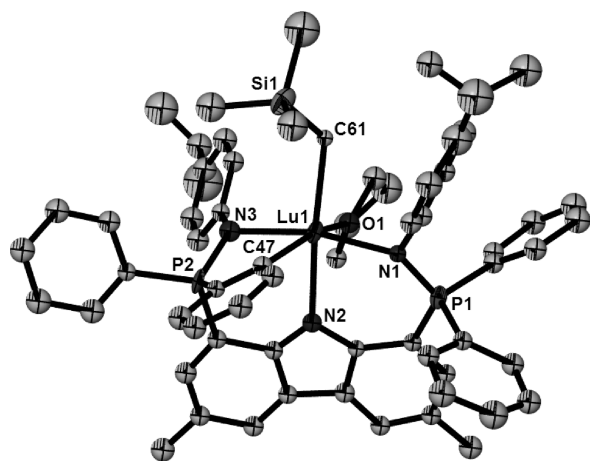


Figure 5. Thermal ellipsoid plot (50% probability) of $\text{LuL}^{\text{Pipp}^*}(\text{CH}_2\text{SiMe}_3)(\text{THF})$ (**6b**) with hydrogen atoms omitted for clarity.

Table 1. Observed Rate Constants for the Intramolecular Metalation of Compounds **5a** and **5b** to **6a** and **6b** at Temperatures Ranging from 282.4 to 326.9 K

compound	T/K	$k_{\text{obs}}/\text{s}^{-1}$	$t_{1/2}/\text{s}$
5a	282.4	1.22×10^{-4}	5690
5a	293.5	4.37×10^{-4}	1590
5a	295.7	5.89×10^{-4}	1180
5a	304.6	1.71×10^{-3}	405
5a	315.7	4.46×10^{-3}	155
5a	326.9	1.55×10^{-2}	44.7
5b	295.7	5.98×10^{-4}	1160

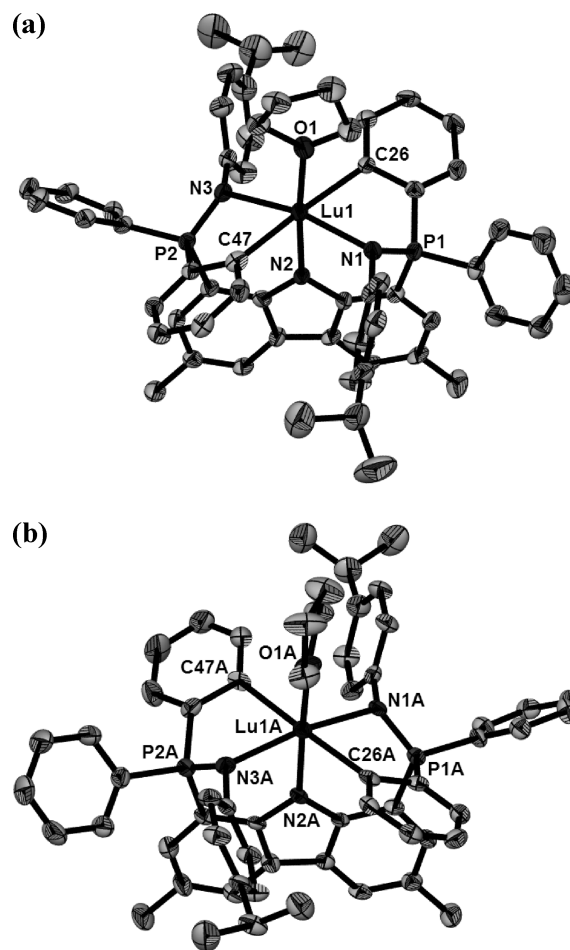


Figure 6. (a) Thermal ellipsoid plot (50% probability) of $\text{LuL}^{\text{Pipp}^*}(\text{THF})$ (**7b**) with hydrogen atoms and solvent molecules of crystallization omitted for clarity. Selected bond distances (Å) and angles (deg): Lu1–N1 = 2.293(6), Lu1–N3 = 2.285(6), Lu1–N2 = 2.343(6), Lu1–C26 = 2.472(8), Lu1–C47 = 2.431(8), Lu1–O1 = 2.30(1), P1–N1 = 1.619(6), P2–N3 = 1.607(7), N1–Lu1–N3 = 166.3(2), C26–Lu1–C47 = 176.4(3), N2–Lu1–O1 = 174.6(4). (b) Thermal ellipsoid plot (50% probability) of $\text{LuL}^{\text{Pipp}^*}(\text{THF})$ (**7b'**) with hydrogen atoms and solvent molecules of crystallization omitted for clarity. Selected bond distances (Å) and angles (deg): Lu1A–N1A = 2.291(6), Lu1A–N3A = 2.298(6), Lu1A–N2A = 2.349(6), Lu1A–C26A = 2.450(8), Lu1A–C47A = 2.425(8), Lu1A–O1A = 2.35(2), P1A–N1A = 1.606(6), P2A–N3A = 1.612(6), N1A–Lu1A–N3A = 167.3(2), C26A–Lu1A–C47A = 178.1(2), N2A–Lu1A–O1A = 174.2(6).

Kinetic Analysis. The decomposition from derivative **5a** to **6a** was quantitatively monitored by $^{31}\text{P}\{^1\text{H}\}$ NMR spectroscopy and revealed to be first order in the dialkyl species. The reaction progress at 293.5 K (from $t = 1760$ s to $t = 15\,500$ s) is depicted in Figure 3 as a stacked plot of $^{31}\text{P}\{^1\text{H}\}$ NMR spectra. As can be seen from the plot, the decreasing concentration of **5a** (δ 29.4) is accompanied by the growth of two broad peaks resonating at δ 27.5 and 22.7 for asymmetric intermediate **6a**. Within 4 h at this temperature complex **6a** gradually converts exclusively to thermodynamic product **7a** (δ 25.6).

The reaction was followed over a broad range of temperatures (282.4 to 326.9 K; Figure 4a), with observed $t_{1/2}$ values ranging from 5690 to 44.7 s (Table 1). Construction of an Eyring plot (Figure 4b) allowed for extraction of the

Table 2. Summary of Crystallography Data Collection and Structure Refinement for Compounds **4a**, **4b**, **6b**, and **7b**

	4a^a	4b^b	6b	7b^c
formula	C ₅₆ H ₄₇ N ₃ P ₂	C ₆₈ H ₆₅ N ₃ P ₂	C ₆₄ H ₇₀ LuN ₃ OP ₂ Si	C ₁₃₈ H ₁₃₄ Lu ₂ N ₆ O ₂ P ₄
fw/g·mol ⁻¹	823.91	986.17	1162.23	2382.33
cryst syst	triclinic	triclinic	monoclinic	monoclinic
space group	<i>P</i> $\bar{1}$	<i>P</i> $\bar{1}$	<i>P</i> 2 ₁ / <i>n</i>	<i>P</i> 2 ₁ / <i>n</i>
<i>a</i> /Å	9.018(3)	8.9413(6)	10.7680(13)	10.9319(9)
<i>b</i> /Å	14.813(4)	16.6229(12)	21.278(3)	44.979(4)
<i>c</i> /Å	19.162(6)	19.4273(14)	26.917(3)	24.495(2)
α /deg	103.236(4)	77.5770(10)	90	90
β /deg	99.522(4)	80.3780(10)	99.461(2)	99.5860(10)
γ /deg	106.150(4)	78.8940(10)	90	90
volume/Å ³	2320.5(12)	2743.2(3)	6083.3(13)	11876.1(17)
<i>Z</i>	2	2	4	4
<i>D</i> _{calc} /mg·m ⁻³	1.179	1.194	1.269	1.332
μ /mm ⁻¹	0.134	0.124	1.736	1.761
<i>F</i> ₀₀₀	868	1048	2392	4888
cryst size/mm	0.24 × 0.13 × 0.082	0.25 × 0.14 × 0.055	0.19 × 0.17 × 0.072	0.38 × 0.078 × 0.035
cryst color	colorless	pale green	yellow-green	green-yellow
cryst habit	plate	plate	block	needle
θ range/deg	1.59–26.37	1.82–25.03	2.14–20.82	1.69–26.37
<i>N</i>	31 432	33 540	68 237	158 092
<i>N</i> _{ind}	9473	9677	6349	24 286
completeness to $\theta = 27.10^\circ$	99.7%	99.8%	99.7%	99.9%
<i>T</i> _{max} ; <i>T</i> _{min}	0.7456; 0.6744	0.7456; 0.6894	0.7456; 0.6019	0.7456; 0.6455
data/restraints/params	9473/0/553	9677/2/664	6349/4/318	24 286/7/1299
GoF on <i>F</i> ²	0.809	1.033	1.060	1.111
<i>R</i> ₁ ^d (<i>I</i> > 2 σ (<i>I</i>))	0.0763	0.0518	0.0994	0.0790
<i>wR</i> ₂ ^e (<i>I</i> > 2 σ (<i>I</i>))	0.1221	0.1232	0.2487	0.1395
$\Delta\rho_{\max}$ and $\Delta\rho_{\min}$ /e·Å ⁻³	0.259; -0.260	0.470; -0.411	5.600; -2.051	2.559; -2.021

^a Crystallized with one molecule of benzene in the asymmetric unit. ^b Crystallized with two molecules of benzene in the asymmetric unit. ^c Crystallized with two independent molecules of **7b**, three molecules of benzene, and one disordered molecule of pentane in the asymmetric unit; ^d $R_1 = \sum |F_o| - |F_c| / \sum |F_o|$. ^e $wR_2 = \{ \sum [w(F_o^2 - F_c^2)^2] / \sum [w(F_o^2)^2] \}^{1/2}$.

activation parameters, $\Delta H^\ddagger = 19.2(2)$ kcal·mol⁻¹ and $\Delta S^\ddagger = -8.2(2)$ cal·K⁻¹·mol⁻¹, for the metalation process. These values correspond to that expected for a highly ordered four-centered transition state^{16,19} and agree well with others reported for intramolecular σ -bond metathesis reactions.²⁰

Kinetic data for the conversion of **6a** to **7a** was not ascertained due to problems in accurately determining the concentration of **6a** over the course of decomposition. Such difficulty stemmed from the broad peaks for **6a** in the ³¹P-¹H NMR spectra, which could not be reproducibly integrated due to the low signal-to-noise ratio. In addition, certain temperature ranges gave rise to an overlap of resonances for **6a** and **7a**. As such, the sum of the concentration of **6a** and **7a** could be readily determined at those temperatures; however, it was not always possible to establish the concentration of each individual species without introducing significant error.

At 295.7 K, metalation of **5a** proceeds at a rate of 5.89×10^{-4} s⁻¹, while that for **5b** was found to be 5.98×10^{-4} s⁻¹ (Table 1). The high degree of correlation between these two rates suggests that the presence of the isopropyl groups in the *para* positions of the *N*-aryl rings of **5b** does not significantly alter reactivity. This result was anticipated, as the incorporation of isopropyl groups on **5b** was intended solely for the purposes of (a) increasing solubility, (b) increasing crystallinity, and (c) providing more diagnostic ¹H NMR

resonances for the *N*-aryl ring compared to that available for **5a**. Furthermore, the solid state structures of proteo ligands, **4a** and **4b**, which were used to prepare **5a** and **5b**, were essentially isostructural (*vide supra*).

Solid State Structures. In order to unambiguously establish that the C–H bond activation of the ancillary ligand occurred through the *ortho* carbon of the phenyl rings on phosphorus, single-crystal X-ray diffraction studies were performed. Crystals of **6b** were serendipitously obtained from an *in situ*-generated solution of **5b** in a 4:1 mixture of toluene and THF at -35 °C over the course of ~1 week. As **5b** slowly decomposed at this temperature, intermediate **6b** selectively crystallized out of solution. Under these dynamic and highly variable conditions the single crystallinity of **6b** was of low quality, and repeated attempts to grow higher quality crystals of this unstable intermediate were unsuccessful. Despite the challenges encountered with crystal quality, a reliable set of low-intensity single-crystal data was obtained for complex **6b**. Such data were sufficient for unambiguously establishing the connectivity of the structure; however, no meaningful comments on the metrical parameters can be made at this time.

A thermal ellipsoid plot of **6b** is depicted in Figure 5. The solid state structure confirms that the ligand is bound to lutetium in a κ^4 -fashion, binding through three nitrogen atoms, as well as via an *ortho* carbon of one *P*-phenyl ring. One trimethylsilylmethyl group remains attached to lutetium as well as one THF donor, giving rise to a structure with distorted octahedral geometry. This structural information corroborates the postulated intermediate in the conversion of dialkyl complex **5b** to diaryl species **7b** (Scheme 3). Due to the very small (< 10 mg) crop of crystals obtained from the crystallization of **6b**, insufficient material was available for further characterization.

(19) Thompson, M. E.; Baxter, S. M.; Bulls, A. R.; Burger, B. J.; Nolan, M. C.; Santarsiero, B. D.; Schaefer, W. P.; Bercaw, J. E. *J. Am. Chem. Soc.* **1987**, *109*, 203–219.

(20) (a) Hayes, P. G.; Piers, W. E.; Parvez, M. *Organometallics* **2005**, *24*, 1173–1183. (b) Conroy, K. D.; Hayes, P. G.; Piers, W. E.; Parvez, M. *Organometallics* **2007**, *26*, 4464–4470. (c) Hayes, P. G.; Piers, W. E.; Lee, L. W. M.; Knight, L. K.; Parvez, M.; Elsegood, M. R. J.; Clegg, W. *Organometallics* **2001**, *20*, 2533–2544.

In contrast to the unstable nature of **6b**, diaryl lutetium **7b** can easily be prepared on a multigram scale. Reaction of **4b** with $\text{Lu}(\text{CH}_2\text{SiMe}_3)_3(\text{THF})_2$ in benzene for 18 h at ambient temperature generated **7b**, which was isolated as a pure yellow crystalline solid. Recrystallization from a benzene solution layered with pentane at ambient temperature afforded large needles of **7b**, which were suitable for X-ray diffraction. It was found that complex **7b** crystallized with two independent molecules in the asymmetric unit, in addition to a variety of solvent molecules. These independent structures, **7b** and **7b'**, are enantiomers of one another and are depicted as thermal ellipsoid plots in Figure 6a and b, respectively.

At $\sim 1.61 \text{ \AA}$, complexes **7b** and **7b'** exhibit P–N bonds that are elongated relative to that of the free ligand (average P–N = 1.575 \AA). Such lengthening is indicative of strong donation from the phosphinimine functionality to the metal center; however, such a distance is still consistent with a formal phosphorus–nitrogen double bond.^{11c} The Lu–C_{aryl} contacts in **7b** and **7b'** range from $2.425(8) \text{ \AA}$ in **7b'** to $2.472(8) \text{ \AA}$ in **7b**. These values fall within the normal range for neutral Lu–C_{aryl} bonds.^{11a,b,18,21} Complexes **7b** and **7b'** both exhibit distorted octahedral geometry at the lutetium center, with the ancillary ligand occupying five of the six coordination sites. The sixth site composing the octahedron is occupied by a THF donor. No attempt has yet been made to remove or exchange the coordinated Lewis base. Future work will explore such processes and investigate the exciting possibility that **7b** may serve as a low-valent (Lu(I)) synthon (via metalation reversal promoted by reaction with reagents of the form H_2ER or H_2SiR_2 (E = N, P; R = sterically bulky group)).²²

Concluding Remarks

In summary, the synthesis and characterization of a versatile family of pincer ligands, which represent a new platform for stabilizing low-coordinate, electronically unsaturated organometallic species, have been described. These carbazole-based ligands have been utilized to prepare monomeric base-free dialkyl lutetium complexes. Although these highly electrophilic complexes are thermally sensitive and undergo a rare double-metalative mechanism with the *ortho* C–H bonds of the *P*-phenyl rings, it is likely that minor structural modifications will yield complexes that are sufficiently stable to allow full exploration of their organometallic chemistry. As such, we are currently reducing the steric bulk around the peripheral edge of the ligand. It is anticipated that replacement of the phenyl groups attached to phosphorus with a less bulky moiety will dampen undesired metalation pathways.

(21) (a) Rufanov, K. A.; Müller, B. H.; Spannenberg, A.; Rosenthal, U. *New J. Chem.* **2006**, *30*, 29–31. (b) Wayda, A. L.; Rogers, R. D. *Organometallics* **1985**, *4*, 1440–1444. (c) Protchenko, A. V.; Almazova, O. G.; Zakharov, L. N.; Fukin, G. K.; Struchkov, Y. T.; Bochkarev, M. N. *J. Organomet. Chem.* **1997**, *536*, 457–463. (d) Rabe, G. W.; Zhang-Prese, M.; Riederer, F. A.; Incarvito, C. D.; Golen, J. A.; Rheingold, A. L. *Acta Crystallogr., Sect. E: Struct. Rep. Online* **2004**, *60*, m1389–m1390. (e) Hogerheide, M. P.; Grove, D. M.; Boersma, J.; Jastrzebski, J. T. B. H.; Kooijman, H.; Spek, A. L.; van Koten, G. *Chem.—Eur. J.* **1995**, *1*, 343–350. (f) Gao, W.; Cui, D. *J. Am. Chem. Soc.* **2008**, *130*, 4984–4991.

(22) (a) Roering, A. J.; Maddox, A. F.; Elrod, L. T.; Chan, S. M.; Ghebream, M. B.; Donovan, K. L.; Davidson, J. J.; Hughes, R. P.; Shalumova, T.; MacMillan, S. N.; Tanski, J. M.; Waterman, R. *Organometallics* **2009**, *28*, 573–581. (b) Mork, B. V.; Tilley, T. D. *J. Am. Chem. Soc.* **2004**, *126*, 4375–4385.

Experimental Section

General Procedures. All reactions were carried out under an argon atmosphere with the rigorous exclusion of oxygen and water using standard glovebox (MBraun) or high vacuum line techniques, unless specified otherwise. The solvents THF, diethyl ether, dichloromethane (DCM), pentane, benzene, and toluene were dried and purified using a solvent purification system (MBraun) and stored in evacuated 500 mL bombs over sodium benzophenone ketyl (THF and ether), CaH_2 (DCM), or “titanocene” (pentane, benzene, and toluene). Deuterated solvents were dried over sodium benzophenone ketyl (benzene-*d*₆ and toluene-*d*₈) or CaH_2 (CDCl_3), degassed via three freeze–pump–thaw cycles, distilled under vacuum, and stored in glass bombs under argon. Unless otherwise specified, all solvents required for air-sensitive manipulations were introduced directly into the reaction flasks by vacuum transfer with condensation at $-78 \text{ }^\circ\text{C}$. For air-stable manipulations, the solvents THF, diethyl ether, DCM, and *n*-hexane were purchased from EMD Chemicals and used without further purification. Samples for NMR spectroscopy were recorded on a 300 MHz Bruker Avance II (Ultrasield) spectrometer (^1H 300.138 MHz, ^{13}C –{ ^1H } 75.468 MHz, ^{31}P { ^1H } 121.495 MHz) and referenced relative to either SiMe_4 through the residual solvent resonance(s) for ^1H and ^{13}C { ^1H } or external 85% H_3PO_4 for ^{31}P { ^1H }. All NMR spectra were recorded at ambient temperature (295 K) unless specified otherwise. FT-IR spectra were recorded on a Bruker ALPHA FT infrared spectrometer with Platinum ATR sampling. Elemental analyses were performed using an Elementar Americas Vario MicroCube instrument. Phenyl azide,²³ 1,8-dibromo-3,6-dimethylcarbazole,¹³ and $\text{Lu}(\text{CH}_2\text{SiMe}_3)_3(\text{THF})_2$ ²⁴ were prepared according to literature procedures. The compound 4-isopropylphenyl azide was prepared according to a modified literature procedure.²⁵ Chlorodiphenylphosphine was purchased from Strem Chemicals and used as received. All deuterated solvents were purchased from Cambridge Isotope Laboratories. All other reagents were obtained from Aldrich Chemicals or Alfa Aesar and used as received.

4-Isopropylphenyl Azide. Aqueous 5 M HCl (125 mL) was added dropwise to a clear dark red solution of 4-isopropylaniline (10.0 g, 74.2 mmol) in THF (100 mL) at $0 \text{ }^\circ\text{C}$. The red-brown solution was stirred for 15 min, following which a solution of NaNO_2 (5.63 g, 81.6 mmol) in H_2O (65 mL) was added dropwise over 20 min. Urea (0.708 g, 11.8 mmol) was added as a solid to remove excess nitrous acid. A solution of NaN_3 (5.65 g, 87.0 mmol) in H_2O (50 mL) was added very slowly at $0 \text{ }^\circ\text{C}$, after which the solution was stirred at this temperature for a further 2 h. The product was extracted into Et_2O ($3 \times 100 \text{ mL}$), and the organic layer was washed with $1 \times 100 \text{ mL}$ of 1 M HCl, dried over MgSO_4 , and concentrated *in vacuo* to give a dark red liquid. The product was purified by filtration through a silica column (20 cm), eluting with hexane. The hexane was removed from the eluent by rotational evaporation, leaving PippN_3 as a canary yellow liquid. Yield: 10.4 g (86.7%). ^1H NMR (CDCl_3): δ 7.21 (d, 2H, $J = 8.4 \text{ Hz}$, Ar–H), 6.96 (d, 2H, $J = 8.4 \text{ Hz}$, Ar–H), 2.90 (sp, 1H, $J = 6.9 \text{ Hz}$, CH), 1.24 (d, 6H, $J = 6.9 \text{ Hz}$, CH_3). ^{13}C { ^1H } NMR (CDCl_3): δ 145.9, 137.5, 127.9, 119.1 (Ar–Cs), 33.7 (CH), 24.2 (CH_3). IR (neat): 2960 (m), 2128 (s), 2092 (s), 1506 (s), 1292 (s), 828 (s), 756 (m), 728 (m), 619 (m), 539 (s) cm^{-1} .

(23) Cwiklicki, A.; Rehse, K. *Arch. Pharm. Pharm. Med. Chem.* **2004**, *337*, 156–163.

(24) (a) Masuda, J. D.; Jantunen, K. C.; Ozerov, O. V.; Noonan, K. J. T.; Gates, D. P.; Scott, B. L.; Kiplinger, J. L. *J. Am. Chem. Soc.* **2008**, *130*, 2408–2409. (b) Estler, F.; Eickerling, G.; Herdtweck, E.; Anwender, R. *Organometallics* **2003**, *22*, 1212–1222. (c) Arndt, S.; Voth, P.; Spaniol, T. P.; Okuda, J. *Organometallics* **2000**, *19*, 4690–4700. (d) Schumann, H.; Freckmann, D. M. M.; Dechert, S. *Z. Anorg. Allg. Chem.* **2002**, *628*, 2422–2426.

(25) Cvrk, T.; Strobel, H. W. *Arch. Biochem. Biophys.* **1998**, *349*, 95–104.

The spectroscopic analysis of this compound agrees with previously published data for the fully characterized product.²⁶

1,8-Dibromo-3,6-dimethyl-9-¹BOC-carbazole (1). An intimate mixture of 1,8-dibromo-3,6-dimethylcarbazole (0.468 g, 1.33 mmol) and dimethylaminopyridine (0.171 g, 1.40 mmol) was dissolved in 30 mL of dichloromethane to give a clear yellow solution. An excess of di-*tert*-butoxycarbonyl (0.479 g, 2.19 mmol) was added via syringe at ambient temperature. The clear red reaction mixture was stirred for 18 h, generating a yellow solution. The reaction was quenched by addition of 50 mL of 1 M HCl. The layers were separated, and the acidic layer was extracted with a further 2 × 50 mL of DCM. The combined fractions were then washed with 3 × 50 mL of 1 M NaHCO₃ followed by 2 × 50 mL of 3 M NaCl. The organic layer was dried over MgSO₄ and filtered, and the solvent was removed under vacuum, giving the N-protected product as an off-white solid. Yield: 0.506 g (84.2%). ¹H NMR (CDCl₃): δ 7.62 (s, 2H, Ar-H), 7.43 (s, 2H, Ar-H), 2.44 (s, 6H, CH₃), 1.68 (s, 9H, OC(CH₃)₃). ¹³C{¹H} NMR (CDCl₃): δ 151.5 (C=O), 137.0, 133.3, 133.1, 127.5, 119.3, 106.2 (Ar-Cs), 86.5 (OC(CH₃)₃), 28.1 (OC(CH₃)₃), 20.9 (CH₃). IR (neat): 2978 (w), 2922 (w), 2860 (w), 1749 (m, ν C=O), 1557 (w), 1478 (m), 1419 (w), 1368 (m), 1309 (m), 1230 (m), 1177 (m), 1127 (s), 1064 (m), 836 (s) cm⁻¹. Anal. Calcd (%) for C₁₉H₁₉Br₂NO₂: C, 50.36; H, 4.23; N, 3.09. Found: C, 49.83; H, 4.17; N, 3.16.

1,8-Bis(diphenylphosphino)-3,6-dimethyl-9-¹BOC-carbazole (2). A pentane solution of ^tBuLi (1.40 mL, 2.38 mmol) was added dropwise to a solution of **1** (0.506 g, 1.12 mmol) in 50 mL of ether at -78 °C, resulting in a cloudy white suspension. The reaction mixture was stirred at -78 °C for 3.5 h, after which an aliquot of chlorodiphenylphosphine (0.425 mL, 2.37 mmol) was slowly added at -78 °C, producing a red-orange color. The solution was allowed to slowly warm to ambient temperature as it was stirred for 16 h, generating a cloudy yellow suspension. The reaction mixture was filtered through a fine-porosity frit to remove insoluble byproducts, and the frit was then washed with ether (2 × 20 mL) until the washings were colorless. The solvent was removed from the filtrate under reduced pressure to yield a gold-colored solid. Recrystallization from a toluene solution layered with pentane at -35 °C gave **2** as an off-white solid. Yield: 0.713 g (96.0%). ¹H NMR (benzene-*d*₆): δ 7.54 (m, 8H, Ph-H), 7.46 (s, 2H, Ar-H), 7.70 (d, 2H, *J* = 4.4 Hz, Ar-H), 7.06 (ov m, 12H, Ph-H), 2.06 (s, 6H, CH₃), 1.40 (s, 9H, OC(CH₃)₃). ¹³C{¹H} NMR (CDCl₃): δ 152.6 (s, C=O), 144.2 (d, *J*_{CP} = 20.9 Hz, Ar-C), 139.0 (d, *J*_{CP} = 14.8 Hz, Ar-C), 135.3 (s, Ar-C), 133.8 (d, *J*_{CP} = 20.4 Hz, Ar-C), 133.2 (s, Ar-C), 128.3 (s, Ar-C), 128.2 (s, Ar-C), 127.8 (d, *J*_{CP} = 5.5 Hz, Ar-C), 126.2 (d, *J*_{CP} = 22.2 Hz, Ar-C), 120.5 (s, Ar-C), 85.5 (s, OC(CH₃)₃), 28.2 (t, *J*_{CP} = 2.6 Hz, OC(CH₃)₃), 21.3 (s, Ar-CH₃). ³¹P{¹H} NMR (benzene-*d*₆): δ -12.0. IR (neat): 3060 (w), 2982 (w), 1724 (s, ν C=O), 1557 (w), 1474 (m), 1434 (m), 1388 (m), 1398 (m), 1277 (m), 1246 (m), 1139 (s), 1090 (m), 1023 (w), 856 (m), 829 (m), 741 (s), 694 (s) cm⁻¹. Anal. Calcd (%) for C₄₃H₃₉NO₂P₂: C, 77.81; H, 5.92; N, 2.11. Found: C, 78.24; H, 6.02; N, 2.39.

1,8-Bis(diphenylphosphino)-3,6-dimethyl-9H-carbazole (3). Toluene (50 mL) was added to a 100 mL bomb charged with **2** (9.33 g, 14.1 mmol) to give a cloudy brown suspension. The bomb was heated to 160 °C for 4.5 h under static vacuum, generating a clear red solution. The product was cannula transferred to a 100 mL round-bottom flask, where the solvent was removed under vacuum to yield an orange solid. Recrystallization from a toluene solution layered with pentane at -35 °C gave **3** as an analytically pure pale yellow solid. Yield: 7.43 g (93.8%). ¹H NMR (benzene-*d*₆): δ 8.36 (s, 1H, NH), 7.81 (s, 2H, Ar-H), 7.37-7.31 (ov m, 10H, Ar-H + PPh-H), 6.98-6.96 (ov m, 12H, PPh-H), 2.26 (s, 6H, CH₃). ¹³C{¹H} NMR (CDCl₃): δ

140.8 (d, *J*_{CP} = 12.9 Hz, Ar-C), 135.7 (d, *J*_{CP} = 9.7 Hz, Ar-C), 133.3 (d, *J*_{CP} = 19.1 Hz, Ar-C), 133.2 (d, *J*_{CP} = 16.1 Hz, Ar-C), 129.0 (d, *J*_{CP} = 6.2 Hz, Ar-C), 128.9-128.7 (ov m, 2 Ar-Cs), 122.9 (m, Ar-C), 121.8 (Ar-C), 117.0 (d, *J*_{CP} = 12.7 Hz, Ar-C), 21.5 (CH₃). ³¹P{¹H} NMR (benzene-*d*₆): δ -15.4. Anal. Calcd (%) for C₃₈H₃₁NP₂: C, 80.98; H, 5.54; N, 2.49. Found: C, 81.19; H, 5.60; N, 2.77.

HL^{Ph} (4a). Benzene (150 mL) was added to a flask charged with **3** (4.73 g, 8.39 mmol) to give a yellow solution. An aliquot of phenyl azide (2.07 g, 17.4 mmol) was added via syringe at ambient temperature. Upon addition, a red product rapidly precipitated out of solution along with concurrent evolution of nitrogen gas. The dark red suspension was stirred under an argon atmosphere for 21 h, following which the solvent was removed under vacuum and the residue brought into a glovebox. The product was washed with 5 × 2 mL of pentane to remove excess azide and dried thoroughly under reduced pressure to afford crude HL^{Ph} as a pale red solid. Recrystallization from a hot benzene solution (20 mL) layered with pentane (15 mL) at ambient temperature generated **4a** as analytically pure pale yellow prisms. Yield: 6.03 g (96.4%). ¹H NMR (CDCl₃): δ 11.8 (s, 1H, NH), 8.01 (s, 2H, Ar-H), 7.69 (m, 8H, PPh-H), 7.46 (t, 4H, *J* = 6.9 Hz, PPh-H), 7.34 (m, 8H, PPh-H), 7.20 (d, 2H, *J* = 14.5 Hz, Ar-H), 6.85 (t, 4H, NPh-H), 6.68 (d, 4H, *J* = 8.0 Hz, NPh-H), 6.58 (t, 2H, *J* = 14.5 Hz, NPh-H), 2.44 (s, 6H, CH₃). ¹³C{¹H} NMR (CDCl₃): δ 151.0 (d, *J*_{CP} = 3.5 Hz, Ar-C), 140.6 (d, *J*_{CP} = 2.9 Hz, Ar-C), 132.9 (d, *J*_{CP} = 9.8 Hz, Ar-C), 131.7 (d, *J*_{CP} = 2.6 Hz, Ar-C), 131.3 (d, *J*_{CP} = 10.5 Hz, Ar-C), 130.8 (d, *J*_{CP} = 89.5 Hz, Ar-C), 128.7 (d, *J*_{CP} = 11.8 Hz, Ar-C), 128.3 (Ar-C), 128.0 (d, *J*_{CP} = 12.7 Hz, Ar-C), 124.2 (d, *J*_{CP} = 2.5 Hz, Ar-C), 123.8 (d, *J*_{CP} = 18.0 Hz, Ar-C), 123.6 (d, *J*_{CP} = 8.5 Hz, Ar-C), 117.3 (Ar-C), 111.6 (d, *J*_{CP} = 118.8 Hz, Ar-C), 21.6 (CH₃). ³¹P{¹H} NMR (CDCl₃): δ 5.4. Anal. Calcd (%) for C₅₀H₄₁NP₂: C, 80.52; H, 5.54; N, 5.63. Found: C, 80.60; H, 5.93; N, 5.37.

HL^{Pipp} (4b). Benzene (75 mL) was added to a flask charged with **3** (2.09 g, 3.71 mmol) to give a light yellow solution. An aliquot of 4-isopropylphenyl azide (1.25 g, 7.72 mmol) was added via syringe at ambient temperature. Upon addition, the solution gradually became a red-orange color with concurrent evolution of nitrogen gas. The solution was stirred under an argon atmosphere for 20 h, following which the solvent was removed under vacuum and the residue brought into a glovebox. The product was recrystallized from hot benzene (15 mL) layered with pentane (5 mL) at ambient temperature. Pale green crystals of **4b** formed over 24 h and were collected by filtration, washed with 2 × 1 mL of pentane, and dried thoroughly under reduced pressure. Yield: 2.17 g (70.4%). ¹H NMR (CDCl₃): δ 11.7 (s, 1H, NH), 8.00 (s, 2H, Ar-H), 7.71 (m, 8H, PPh-H), 7.46 (t, 4H, *J* = 7.4 Hz, PPh-H), 7.33 (m, 8H, PPh-H), 7.23 (d, 2H, *J* = 14.6 Hz, Ar-H), 6.74 (d, 4H, *J* = 8.2 Hz, Pipp-H), 6.64 (d, 4H, *J* = 8.3 Hz, Pipp-H), 2.74 (sp, 2H, *J* = 6.9 Hz, CH(CH₃)₂), 2.45 (s, 6H, CH₃), 1.17 (d, 12H, *J* = 6.9 Hz, CH(CH₃)₂). ¹³C{¹H} NMR (CDCl₃): δ 148.3 (Ar-C), 140.5 (d, *J*_{CP} = 2.9 Hz, Ar-C), 137.5 (Ar-C), 133.0 (d, *J*_{CP} = 9.8 Hz, Ar-C), 131.6 (d, *J*_{CP} = 2.5 Hz, Ar-C), 131.3 (d, *J*_{CP} = 10.9 Hz, Ar-C), 130.9 (d, *J*_{CP} = 87.2 Hz, Ar-C), 128.6 (d, *J*_{CP} = 11.7 Hz, Ar-C), 127.9 (d, *J*_{CP} = 12.8 Hz, Ar-C), 126.2 (Ar-C), 124.1 (d, *J*_{CP} = 2.6 Hz, Ar-C), 123.5 (d, *J*_{CP} = 17.6 Hz, Ar-C), 123.5 (d, *J*_{CP} = 9.0 Hz, Ar-C), 111.9 (d, *J*_{CP} = 120.2 Hz, Ar-C), 33.2 (CH(CH₃)₂), 24.4 (CH(CH₃)₂), 21.6 (CH₃). ³¹P{¹H} NMR (CDCl₃): δ 4.57. Anal. Calcd (%) for C₅₆H₅₃N₃P₂: C, 81.04; H, 6.44; N, 5.06. Found: C, 80.21; H, 6.50; N, 4.98.

LuL^{Ph}(CH₂SiMe₃)₂ (5a). An NMR tube was charged with **4a** (0.0400 g, 0.0536 mmol) and Lu(CH₂SiMe₃)₃(THF)₂ (0.0312 g, 0.0537 mmol) and sealed with a rubber septum and parafilm. The tube was cooled to -78 °C, and an aliquot of toluene-*d*₈ (0.5 mL) was added via syringe. The tube was removed from the cold bath, shaken briefly to mix the reagents, and then immediately inserted into a precooled (271.3 K) NMR probe. The dialkyl

(26) (a) Das, J.; Patil, S. N.; Awasthi, R.; Prasad Narasimhulu, C.; Trehan, S. *Synthesis* **2005**, *11*, 1801-1806.

complex (**5a**) was characterized by multinuclear NMR spectroscopy *in situ*. No decomposition was observed over the course of characterization (2 h). ^1H NMR (toluene- d_8 ; 271.3 K): δ 8.12 (s, 2H, Ar-H), 7.47 (m, 8H PPh-H), 6.93–6.75 (ov m, 24H, Ar-H), 2.29 (s, 6H, CH_3), -0.06 (s, 18H, CH_3), -0.79 (s, 4H, CH_2). $^{13}\text{C}\{^1\text{H}\}$ NMR (toluene- d_8 ; 271.3 K): δ 152.5 (d, $J_{\text{CP}} = 3.6$ Hz, Ar-C), 147.4 (d, $J_{\text{CP}} = 7.4$ Hz, Ar-C), 137.1 (Ar-C), 134.1 (d, $J_{\text{CP}} = 9.4$ Hz, Ar-CH), 132.3 (d, $J_{\text{CP}} = 2.2$ Hz, Ar-CH), 130.9 (d, $J_{\text{CP}} = 11.4$ Hz, Ar-CH), 129.4 (d, $J_{\text{CP}} = 7.9$ Hz, Ar-CH), 129.1 (d, $J_{\text{CP}} = 2.4$ Hz, Ar-CH), 128.6 (d, $J_{\text{CP}} = 11.8$ Hz, Ar-CH), 127.3 (d, $J_{\text{CP}} = 9.3$ Hz, Ar-C), 126.0 (d, $J_{\text{CP}} = 2.2$ Hz, Ar-CH), 125.2 (Ar-C), 123.2 (d, $J_{\text{CP}} = 2.8$ Hz, Ar-CH), 108.9 (d, $J_{\text{CP}} = 111.2$ Hz, Ar-C), 40.4 (CH_2), 21.3 (CH_3), 4.63 (Si(CH_3) $_3$). $^{31}\text{P}\{^1\text{H}\}$ NMR (toluene- d_8 ; 271.3 K): δ 29.6.

LuL^{Pipp}(CH₂SiMe₃)₂ (5b). An NMR tube was charged with **4b** (0.0216 g, 0.0260 mmol) and Lu(CH₂SiMe₃)₃(THF)₂ (0.0152 g, 0.0262 mmol) and sealed with a rubber septum and parafilm. The tube was cooled to -78 °C, and an aliquot of toluene- d_8 (0.5 mL) was added via syringe. The tube was removed from the cold bath, shaken briefly to mix the reagents, and then immediately inserted into a precooled (249.1 K) NMR probe. The dialkyl complex (**5b**) was characterized by multinuclear NMR spectroscopy *in situ*. No decomposition was observed over the course of characterization (3 h). ^1H NMR (toluene- d_8 ; 249.1 K): δ 8.11 (s, 2H, Ar-H), 7.49 (m, 8H PPh-H), 7.11–7.10 (ov m, 4H, Ar-H), 6.96–6.79 (ov m, 18 H, Ar-H), 2.63 (sp, 2H, $\text{CH}(\text{CH}_3)_2$), 2.29 (s, 6H, CH_3), 1.13 (d, $J = 6.6$ Hz, 12H, $\text{CH}(\text{CH}_3)_2$), -0.01 (s, 18H, Si(CH_3) $_3$), -0.72 (s, 4H, CH_2). $^{13}\text{C}\{^1\text{H}\}$ NMR (toluene- d_8 ; 249.1 K): δ 152.5 (d, $J_{\text{CP}} = 3.5$ Hz, Ar-C), 144.8 (d, $J_{\text{CP}} = 7.5$ Hz, Ar-C), 143.4 (d, $J_{\text{CP}} = 3.6$ Hz, Ar-C), 137.0 (Ar-C), 134.1 (d, $J_{\text{CP}} = 9.6$ Hz, Ar-CH), 132.2 (Ar-CH), 130.9 (d, $J_{\text{CP}} = 11.6$ Hz, Ar-CH), 129.2 (Ar-CH), 128.5 (d, $J_{\text{CP}} = 11.7$ Hz, Ar-CH), 127.3 (d, $J_{\text{CP}} = 9.3$ Hz, Ar-C), 127.0 (Ar-CH), 126.0 (Ar-CH), 125.0 (Ar-C), 108.9 (d, $J_{\text{CP}} = 110.6$ Hz, Ar-C), 40.0 (CH_2), 33.9 ($\text{CH}(\text{CH}_3)_2$), 24.5 ($\text{CH}(\text{CH}_3)_2$), 21.3 (CH_3), 4.71 (Si(CH_3) $_3$). $^{31}\text{P}\{^1\text{H}\}$ NMR (toluene- d_8 ; 249.1 K): δ 29.4.

LuL^{Ph}(THF) (7a)**. In a glovebox, a small Erlenmeyer flask was charged with **4a** (0.193 g, 0.259 mmol) and Lu(CH₂SiMe₃)₃(THF)₂ (0.147 g, 0.252 mmol). Benzene (5 mL) was added to this solid mixture at ambient temperature to give a clear dark red solution. The reaction mixture was stirred for 18 h, following which the volatiles were removed to afford a yellow powder. The product was recrystallized from a 9:1 benzene/THF solution (10 mL) layered with pentane (10 mL). The crystals were collected by filtration, washed with pentane (2 mL), and dried under vacuum. Yield: 0.201 g (80.5%). ^1H NMR (benzene- d_6): δ 8.08 (s, 2H, Ar-H), 7.97 (m, 4H, PPh-H), 7.71 (m, 2H, PPh-H), 7.56 (d, 2H, $J = 13.4$ Hz, Ar-H), 7.11–6.97 (ov m, 12H, PPh-H), 6.77 (ov m, 10 H, NPh-H), 4.00 (s, 4H, OCH_2CH_2), 2.34 (s, 6H, CH_3), 1.15 (s, 4H, OCH_2CH_2). $^{13}\text{C}\{^1\text{H}\}$ NMR (benzene- d_6): δ 204.6 (dd, $^2J_{\text{CP}} = 41.2$ Hz, $^4J_{\text{CP}} = 1.1$ Hz, Lu-Ar-C), 151.5 (d, $J_{\text{CP}} = 5.7$ Hz, Ar-C), 147.5 (d, $J_{\text{CP}} = 7.3$ Hz, Ar-C), 140.0 (d, $J_{\text{CP}} = 25.6$ Hz, Ar-CH), 138.5 (d, $J_{\text{CP}} = 126.7$ Hz, Ar-C), 134.2 (d, $J_{\text{CP}} = 8.5$ Hz, Ar-CH), 132.2 (d, $J_{\text{CP}} = 1.7$ Hz, Ar-CH), 129.6 (d, $J_{\text{CP}} = 8.7$ Hz, Ar-CH), 129.1 (d, $J_{\text{CP}} = 2.1$ Hz, Ar-CH), 128.7 (s, Ar-CH), 128.6 (d, $J_{\text{CP}} = 7.2$ Hz, Ar-CH), 128.2 (Ar-CH), 127.8 (d, $J_{\text{CP}} = 3.7$ Hz, Ar-CH), 127.0 (d, $J_{\text{CP}} = 9.8$ Hz, Ar-C), 126.3 (d, $J_{\text{CP}} = 81.5$ Hz, Ar-C), 124.9 (d, $J_{\text{CP}} = 11.3$ Hz, Ar-C), 124.6 (d, $J_{\text{CP}} = 14.7$ Hz, Ar-CH), 124.2 (d, $J_{\text{CP}} = 2.3$ Hz, Ar-CH), 122.6 (d, $J_{\text{CP}} = 3.2$ Hz, Ar-CH), 115.0 (d, $J_{\text{CP}} = 87.0$ Hz, Ar-C), 71.3 (OCH_2CH_2), 25.3 (OCH_2CH_2), 21.5 (CH_3). $^{31}\text{P}\{^1\text{H}\}$ NMR (benzene- d_6): δ 25.9. Anal. Calcd (%) for C₅₄H₄₆LuN₃OP₂: C, 65.52; H, 4.68; N, 4.24. Found: C, 64.47; H, 5.02; N, 3.99.

LuL^{Pipp}(THF) (7b)**. In a glovebox, a small Erlenmeyer flask was charged with **4b** (0.506 g, 0.609 mmol) and Lu(CH₂SiMe₃)₃(THF)₂ (0.354 g, 0.610 mmol). Benzene (5 mL) was added to this solid mixture at ambient temperature to give a clear dark red

solution. The reaction mixture was stirred for 18 h, giving a dark red solution and a small quantity of an orange solid. An aliquot of THF (0.5 mL) was added to redissolve all material, and the clear red solution was then layered with pentane (10 mL) and left at ambient temperature to crystallize. Fine needles developed over 48 h, which were collected by filtration, washed with pentane (2 mL), and dried under vacuum. Yield: 0.252 g (38.5%). ^1H NMR (benzene- d_6): δ 8.14 (s, 2H, Ar-H), 8.00 (m, 4H, PPh-H), 7.72 (m, 2H, PPh-H), 7.57 (d, 2H, $J = 13.4$ Hz, Ar-H), 7.13–6.98 (ov m, 12H, PPh-H), 6.69 (dd, 4H, $J = 8.4$, $J = 2.2$ Hz, Pipp-H), 6.60 (d, 4H, $J = 8.2$ Hz, Pipp-H), 4.04 (s, 4H, OCH_2CH_2), 2.63 (sp, 2H, $J = 6.8$ Hz, $\text{CH}(\text{CH}_3)_2$), 2.37 (s, 6H, CH_3), 1.20 (s, 4H, OCH_2CH_2), 1.14 (d, 6H, $J = 6.9$ Hz, $\text{CH}(\text{CH}_3)(\text{CH}_3')$), 1.12 (d, 6H, $J = 6.9$ Hz, $\text{CH}(\text{CH}_3)(\text{CH}_3')$). $^{13}\text{C}\{^1\text{H}\}$ NMR (benzene- d_6): δ 204.7 (dd, $^2J_{\text{CP}} = 40.9$ Hz, $^4J_{\text{CP}} = 1.2$ Hz, Lu-Ar-C), 151.6 (d, $J_{\text{CP}} = 5.7$ Hz, Ar-C), 144.6 (d, $J_{\text{CP}} = 7.3$ Hz, Ar-C), 142.8 (d, $J_{\text{CP}} = 3.5$ Hz, Ar-C), 140.0 (d, $J_{\text{CP}} = 25.3$ Hz, Ar-CH), 138.5 (d, $J_{\text{CP}} = 127.3$ Hz, Ar-C), 134.2 (d, $J_{\text{CP}} = 8.5$ Hz, Ar-CH), 132.0 (d, $J_{\text{CP}} = 2.2$ Hz, Ar-CH), 129.7 (d, $J_{\text{CP}} = 8.6$ Hz, Ar-CH), 128.8 (d, $J_{\text{CP}} = 24.7$ Hz, Ar-CH), 128.3 (d, $J_{\text{CP}} = 4.8$ Hz, Ar-CH), 128.1 (Ar-CH), 127.6 (d, $J_{\text{CP}} = 3.9$ Hz, Ar-CH), 127.1 (d, $J_{\text{CP}} = 2.5$ Hz, Ar-CH), 126.9 (d, $J_{\text{CP}} = 0.96$ Hz, Ar-C), 126.7 (d, $J_{\text{CP}} = 81.3$ Hz, Ar-C), 124.9 (d, $J_{\text{CP}} = 11.3$ Hz, Ar-C), 124.5 (d, $J_{\text{CP}} = 14.8$ Hz, Ar-CH), 124.1 (d, $J_{\text{CP}} = 2.0$ Hz, Ar-CH), 115.4 (d, $J_{\text{CP}} = 86.2$ Hz, Ar-C), 71.2 (OCH_2CH_2), 33.9 ($\text{CH}(\text{CH}_3)_2$), 25.4 (OCH_2CH_2), 24.5 ($\text{CH}(\text{CH}_3)(\text{CH}_3')$), 24.5 ($\text{CH}(\text{CH}_3)(\text{CH}_3')$), 21.5 (CH_3). $^{31}\text{P}\{^1\text{H}\}$ NMR (benzene- d_6): δ 25.0. Anal. Calcd (%) for C₆₀H₅₈LuN₃OP₂: C, 67.10; H, 5.44; N, 3.91. Found: C, 67.07; H, 6.02; N, 3.64.

NMR Kinetics. All rate constants were determined by monitoring the $^{31}\text{P}\{^1\text{H}\}$ NMR resonance(s) over the course of the reaction (to at least 3 half-lives) at a given temperature. In a typical experiment, proteo ligand **4a** (0.0400 g, 0.0536 mmol) and Lu(CH₂SiMe₃)₃(THF)₂ (0.0312 g, 0.0537 mmol) were added to a Wilmad NMR tube, which was then sealed with a rubber septum (Sigma-Aldrich) and parafilm. The tube was cooled to -78 °C and 0.5 mL of toluene- d_8 was injected via syringe. The tube was removed from the cold bath and shaken briefly, generating LuL^{Ph}(CH₂SiMe₃)₂, **5a**, *in situ*. The tube was then immediately inserted into the NMR probe, which was pre-equilibrated to the appropriate temperature. The sample was allowed to equilibrate at the set temperature over the course of shimming the tube in the magnet. $^{31}\text{P}\{^1\text{H}\}$ NMR spectra (16 scans) were recorded at preset time intervals until the reaction had progressed to at least 3 half-lives. The extent of reaction at each time interval was determined by integration of the peak intensity of the starting material relative to that of the intermediate and product. An appropriately long delay between scans was utilized to ensure that integration was quantitative and not affected by the T_1 relaxation times of the reacting species. A summary of the observed rate constants and half-lives is listed in Table 1.

X-ray Crystallography. Suitable crystals of **4a**, **4b**, **6b**, or **7b** were selected, coated in dry Paratone oil, and mounted on a glass fiber. Data were collected at 173 K using a Bruker SMART APEX II instrument (Mo K α radiation, $\lambda = 0.71073$ Å) equipped with a CCD area detector and a KRYO-FLEX liquid nitrogen vapor cooling device. Unit cell parameters were determined and refined on all observed reflections using APEX2 software.²⁷ Data reduction and correction for Lorentz polarization were performed using the SAINT-Plus software.²⁸ Absorption corrections were applied using SADABS.²⁹ The structure was solved by Patterson (**4a**) or direct (**4b**, **6b**, and **7b**) methods and refined by the least-squares method on F^2 using the

(27) APEX2, version 2.1-4; Data Collection and Refinement Program; Bruker AXS: Madison, WI, 2006.

(28) SAINT-Plus, version 7.23a; Data Reduction and Correction Program; Bruker AXS: Madison, WI, 2004.

(29) Sheldrick, G. M. SADABS, version 2004/1; Program for Empirical Absorption Correction; Bruker AXS: Madison, WI, 2004.

SHELXTL program package.³⁰ Details of the data collection and refinement are given in Table 2 and the Supporting Information.

Acknowledgment. P.G.H. acknowledges financial support from the Natural Sciences and Engineering Research Council of Canada for a Discovery Grant, the Canada

(30) (a) Sheldrick, G. M. *SHELXTL, version 6.14; Structure Determination Software Suite*; Bruker AXS: Madison, WI, 2003. (b) Sheldrick, G. M. *Acta Crystallogr., Sect. A: Found. Crystallogr.* **2008**, *A64*, 112–122.

Foundation for Innovation for a Leaders Opportunity Grant, and the University of Lethbridge for a start-up fund. The authors also wish to thank Dr. Adrien Côté (Xerox Canada) for expert assistance with X-ray crystallography and Mr. Craig Wheaton of this department for performing elemental analyses.

Supporting Information Available: X-ray crystallographic data in PDF format and CIF files are available free of charge via the Internet at <http://pubs.acs.org>.